

Related Reviews: Multiband Planar Inverted Antenna for Mobile Communication

Erfan Rohadi¹, Puteri Nurul Ma'rifah¹, Andari Dyah Widowatie¹, Mochammad Junus¹, and Indrazno Siradjuddin¹

¹*Department of Electrical Engineering, Malang State Polytechnic, Indonesia*

Corresponding Author: Puteri Nurul Ma'rifah, pnurulmarifah@gmail.com

Received Date: 13-10-2022

Revised Date: 13-11-2022

Accepted Date: 01-12-2022

Abstract

Research in the field of planar inverted antennas with multiband frequencies is currently being developed. Due to the hugely increased number of mobile users, at least every time a new generation is released, a mobile communication system is released with additional features. All additional features of a mobile communication system require an antenna that resonates over a specific frequency spectrum range, meaning multiple antennas are required in a single mobile device to function across all generations for all frequency spectrums. To reduce the number of antennas on a mobile communication system device, it is necessary to design a new type of antenna that operates in a different frequency range. The inverted planar multiband antenna is designed to have changing sizes, shapes, and material properties. Types of inverted planar antennas include planar inverted-L antennas (PILA) and planar inverted-F antennas (PIFA). After analysis, the antenna designed by Juan Zhang et al. is the best solution for mobile communication systems. The designed antenna has compact antenna dimensions and four frequency bands that can be applied to N1/N78/N79 5G and 5.8 GHz WLAN. The antenna has a high gain of almost 5dB in the 5.60–7.00 GHz frequency range. They also claim that the antenna has a beam efficiency of four very high-frequency antenna points and a small side lobe that appears only at the top at the highest frequency point. But unfortunately, the antenna cannot cover the entire frequency range that must exist in a mobile communication system.

Keywords : Antenna Design, Antenna Compact, Frequency Spectrum, Multiband Antenna

1 Introduction

Extraordinary advancements in mobile communication technology, combined with consumer growth, result in the development of smaller, lighter, and more multifunctional mobile handsets [1], [2]. This encourages the development of antennas from single-band to multi-band, as well as the design of ultra-wideband antennas with a compact size, lightweight, low cost, and ease of manufacture/integration in mobile devices [1], [3]. The needs of mobile communication that can be used, smartphones designed with thin, lightweight, multi-band and high gain antennas and other characteristics of smart phones have become a challenge for the design of the new generation of mobile phones today.

Miniaturization of internal antennas for mobile devices is also an inevitable trend, and over the past ten years, a large number of antenna designers have conducted many studies [1], [4]. But the realization of a small antenna size is difficult to do because the LTE 700 wavelength is quite long, especially when the antenna operating frequency band is asked to cover all 2G/3G/4G/5G standard communication bands at this time, such as LTE 700 (698-787 MHz), GSM 850 (824-894 MHz), GSM 900 (880-960 MHz), DCS1800 (1710-1880MHz), PCS1900 (1850-1990MHz), UMTS (1920-2170 MHz), LTE 2300 (2300-2400 MHz) and LTE 2500 (2500-2690 MHz), NR (Sub-1 GHz, 1-6 GHz and above 6 GHz), Bluetooth (2400-2480 MHz), WLAN (2400-2484MHz, 5150-5350 MHz and 5725-5825 MHz) and others so on will be a greater challenge [1], [5].

Therefore, the antenna is expected to meet current technological development requirements. The antenna must be compact and have multiband capabilities. At present, attention is being focused on high-performance antennas with simple structures to achieve and meet the requirements. Various techniques for multiband antenna design based on different structures have been proposed. One of the antennas that is being developed for mobile communication applications is the planar inverted antenna. Planar Inverted-L Antenna (PILA) and Planar Inverted-F Antenna (PIFA) are two types of inverted planar antenna. Several designs of planar inverted-L/inverted-F antennas with usable frequencies have been reported [6]–[11]. Some of the techniques used to design the planar inverted-L/inverted-F antenna reported so far include a quarter-circle sector with an inverted L-shaped monopole antenna for tri-band applications [6], Multiple bands are generated using a cactus-shaped patch, consisting of inverted L-shaped slots and L-shaped branches [7], A miniaturized Rectangular Monopole Antenna (RMA) integrated with T-shaped stub, inverted long and short L-shaped stub resonators based on the application of Characteristic Mode theory (CM) were investigated for multiband operation [8], a compact Ultra-Wideband (UWB) antenna with an antenna structure, i.e. two open-ended inverted L-shaped slots carved into a square ground plane [9], then in [10], a proposed an inverted-F-printed dual-band antenna with a nested structure, and a dual-band capacitive paired planar inverted F antenna [11].

Research in the field of planar inverted antennas with usable frequencies for mobile communication technology is ongoing but requires a good review to make planar inverted antenna designers familiar with the state of the recent developments in planar inverted antennas. This paper attempts to provide an overview of the requirements and challenges, as well as various techniques used to fulfill them, in the field of inverted planar antennas for mobile communication technology.

2 Method

2.1 Antena Design

Various techniques for designing planar inverted antennas based on different structures for mobile communication technology have been proposed. Key types are discussed in this section.

2.1.1 Planar Inverted-L Antenna (PILA)

The Planar Inverted-L Antenna (PILA) was one of the earliest low-profile antennas. It was found to be a promising candidate as an antenna with its low profile and simple structure. However, PILA has a low input resistance and high input reactance caused by the horizontal top plate, thus experiencing high mismatch losses, which makes it less attractive for small and low-profile antenna designs. To overcome this problem, the traditional solution that is usually used is to modify the PILA structure [13]. PILA consists of a ground plane, radiator, feed line, and short pin. Patch size and resonant frequency can be determined by [1], [14]:

$$L_p + W_p - W = \frac{\lambda}{4} \quad (1)$$

$$f_r = \frac{C}{4(L_p + W_p - W)\sqrt{\epsilon_r}} \quad (2)$$

Where L_p -patch length, W_p -patch width, W -width of shorting line, ϵ_r -dielectric permittivity, C -speed of light. Because it operates at a resonant length of $\lambda/4$, it is highly conducive to a small and lightweight design [1].

Recently, many researchers are working on PILA antennas. A compact Triple-band PILA antenna is proposed [6], to cover the frequency range of the 2.1–2.485 GHz band for Bluetooth (2.402–2.482 GHz), 3G, Wi-Fi (2,400–2.483 GHz), LTE 2300 (2.305–2.400 GHz), 5.05–5.67 GHz band for WLAN applications, and 8.4–9.0 GHz band for applications in the X-band with the proposed antenna geometry shown in Figure 1(a). The antenna structure consists of a quarter-circle sector and a rectangular inverted L strip. To provide a capacitive effect and achieve the desired tri-band, a similarly shaped parasitic element is placed close to the radiator. To improve impedance matching, a small part of the circle arcs to the right of the feed line. The detailed antenna dimensions are = 32 mm, = 21 mm, = 10 mm, = 19 mm, = 1 mm, = 10 mm, = 9 mm, = 8 mm, = 7 mm, = 8 mm, = 6 mm, = 3 mm, = 7 mm, = 1 mm, = 1 mm, and = 3 mm. The antenna is designed on a 1.6 mm thick FR4 substrate with the dielectric constant and loss tangent of the FR4 substrate being 4.4 and 0.02, respectively, and the antenna is fed through a 50 microstrip line. Structure The antenna occupies a board area of $32 \times 21 \text{ mm}^2$.

A Compact Four-Band Cactus-Shaped Antenna is proposed [7], with a cactus-shaped patch antenna structure with an inverted L-shaped slot and an L-shaped prong used as a radiator to create four operating bands,

covering the 5G band N1/N78/N79 (2.11 GHz–2.17 GHz, 3.3 GHz–3.8 GHz, 4.4 GHz–5.0 GHz) and 5.8 GHz WLAN bands (5.725 GHz–5.825 GHz) with the proposed antenna geometry shown in Figure 1(b), where it can be seen that the radiator and ground plane were printed on a 1.6 mm thick FR4 dielectric substrate (relative permittivity 4.4, and loss tangent 0.02).

Table 1: Review Of The Design PILA

No.	Ref	Antenna Size ($W \times L \times h$ mm ³)	Dielectric Materials	ϵ_r	$\tan \delta$	Design Type	Operating band (GHz)	Antenna Response	Application
1	[6]	$32 \times 21 \times 1.6$	FR-4	4.4	0.02	A quarter circular sector and a rectangular inverted L strip	2.10–2.48 5.05–5.67 8.40–9.00	Triple-band	3G, Wi-Fi, LTE, Bluetooth, WLAN, and X-band
2	[7]	$21 \times 29 \times 1.6$	FR4	4.4	0.02	A cactus-shaped patch with inverted L-shaped slots and L-shaped branches	2.10–2.25 3.24–3.65 4.42–5.44 5.60–7.00	Four-band	5G (N1/N78/N79) and WLAN
3	[8]	$20 \times 30 \times 0.79$	Rogers RT/duroid 5880	2.2	0.0009	A T-shaped stub resonator with inverted long and short L-shaped stub resonators	2.47–2.65 3.27–3.63 5.20–5.83	Triple-band	WiMAX, and WLAN
4	[9]	$28 \times 28 \times 1.6$	FR4	4.4	0.02	Two open ended rounded inverted L-shaped slots are etched on the square ground plane	2.7–12.55	Ultra-wideband	UWB

The geometry of the substrate is $21 \times 29 \times 1.6$ mm³, which is a rectangular solid. The proposed microstrip antenna is fed by a coplanar waveguide and the SMA connector impedance in our work is 50ω , so we have designed the feed line to be 50 as well. The calculated width for the feed line is 3.5 mm, and the gap is 0.5 mm to obtain a 50 impedance match. All antenna parameters are $= 29$ mm, $= 12$ mm, $= 5.4$ mm, $= 3$ mm, $= 9$ mm, $= 9.5$ mm, $= 14.4$ mm, $= 13.4$ mm, $= 7.8$ mm, $= 2$ mm, $= 21$ mm, $= 8.25$ mm, $= 3.5$ mm, $= 0.6$ mm, $= 1.2$ mm, $= 0.8$ mm, $= 0.3$ mm, $= 5.9$ mm, $= 7.8$ mm, $= 0.9$ mm, $= 0.6$ mm, and $= 1$ mm.

Another PILA antenna is proposed [8], such as Figure 1(c) illustrating the proposed configuration of a multi-stub charged planar monopole antenna designed on a low-loss Rogers RT/duroid 5880 dielectric substrate having a dielectric constant (ϵ_r) of 2.2, a thickness of 0.79 mm, and the loss tangent is 0.0009. The antenna consists of a 50 microstrip feed line with a width of w , a small rectangular patch $a \times b$, a T-shaped stub resonator, a long and short inverted L-shaped stub resonator of the same width $d = 1.5$ mm on the front side, and a partial ground plane $c \times d$ on the back side of the substrate. Embeds three-quarters ($3/4$) guided wavelength stub resonator vertically (along the y-axis) with different g_1 and g_2 gaps on the top contour of the rectangular patch. This is attributed to a different triple resonance, much smaller size, and simple different configuration. The antenna size is 20×30 mm² ($0.17\lambda_0 \times 0.26\lambda_0$, where λ_0 is the free space wavelength at 2.6 GHz). The optimal values of the planar structure are $= 30$ mm, $= 4.5$ mm, $= 5$ mm, $= 17.8$ mm, $= 12.3$ mm, $= 6.15$ mm, $= 20$ mm, $= 8$ mm, $= 2.44$ mm, $= 5$ mm, $= 5.3$ mm, $= 4.5$ mm, $= 1.7$ mm, and $= 1.8$ mm. This antenna is best suited for WiMAX 2.5/3.5/5.5 GHz and 5.2/5.8 GHz WLAN applications

for Ultra-Wideband (UWB), where UWB is a radio technology used for various frequency channels and has low short-distance energy. This is used for short-distance wireless communication protocols such as Bluetooth and Wi-Fi.

2.1.2 Planar Inverted-F Antenna (PIFA)

The Planar Inverted F-Antenna (PIFA) is developed from a monopole antenna, i.e., the inverted L is realized by folding the monopole to reduce the antenna height while maintaining an identical resonant length. When a feed is applied to an inverted L, it appears as an inverted F antenna. To obtain a planar inverted F antenna, the thin top wire of the inverted F is replaced by planar elements [1], [15]. Like PILA, PIFA also consists of a ground plane, radiator, feed line, and short pin. To reduce the length of the antenna, the top radiating patch plane is folded at one edge of the patch and shortened to the base plane [1], [14], [15].

A dual-band PIFA antenna is proposed [10] to cover the frequency bands of 2.50-2.62 GHz and 5.28-5.78 GHz for WLAN applications, and the antenna is designed by selecting the parameters $l_1a, l_1b, h_1, l_2a, l_2b, h_2$, and line width as shown in Figure 2(a). The antenna is designed on an FR-4 (Panasonic R-1705) substrate, and the antenna is fed through a 50 microstrip line with a signal line of 3 millimeters wide. The antenna structure consists of two F-shaped patterns nested in the top metal layer. Shorter elements are used for higher frequency bands and longer ones for lower bands. Two via holes with a diameter of 1.27 mm are used to connect the top and bottom metal layers. The Sub-Miniature version A (SMA) connector is attached to the edge of the substrate (shown in Figure 2(b)) used for measurement. The antenna structure occupies a board dimension area of $30 \times 22 \times 1.57 \text{ mm}^3$.

Table 2: Review Of The Design PIFA

No.	Ref	Antenna Size ($W \times L \times h$ mm ³)	Dielectric Materials	ϵ_r	$\tan \delta$	Design Type	Operating band (GHz)	Antenna Response	Application
1	[10]	$30 \times 22 \times 1.57$	FR-4	4.3	0.015	A dual-band printed inverted-F antenna	2.50-2.62 5.28-5.78	Dual-band	WLAN
2	[11]	$10 \times 40 \times 6$	FR-4	4.4	0.02	A compact capacitive coupled dual-band PIFA	1.5 2.4	Dual-band	GPS and WLAN

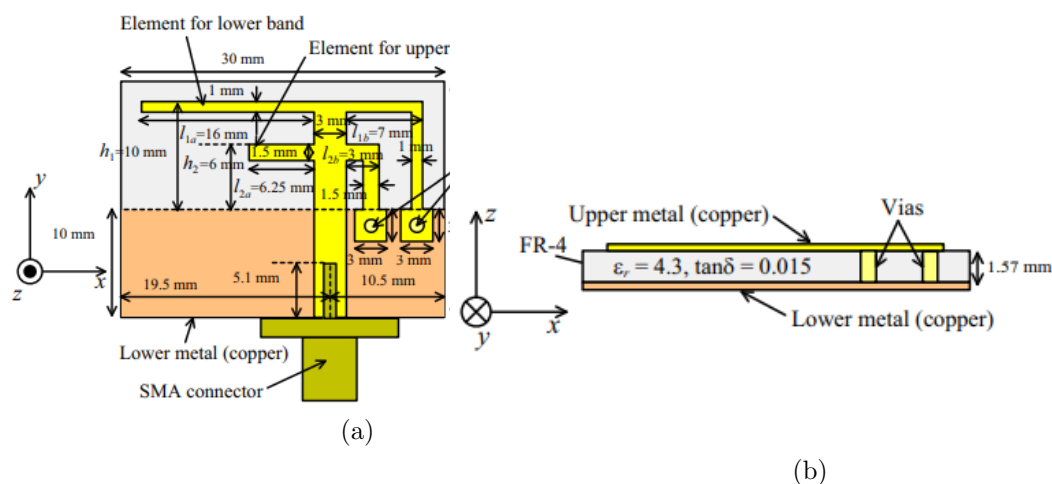


Figure 2: Configuration of the dual-band printed inverted-F antenna. (a) Top view. (b) Cross sectional.

Another PIFA antenna is proposed [11], as illustrated in Figure 3(a), which depicts the fabrication structure and geometry of a capacitively coupled dual-band PIFA antenna. The antenna consists of a metal top plane and a ground plane system, It is excited by a single probe feed connected to a square capacitive strip. In the upper plane, the antenna also consists of an L-shaped slotted line, and it is suspended above the ground plane and shortened to the ground plane by a short metal plane. The antenna is designed on an FR-4 dielectric substrate. The optimized antenna design parameters are $W_t = 10$ mm, $L_t = 34.5$ mm, $L_h = 13.5$ mm, $L_v = 5$ mm, $h = 6$ mm, $W_g = 40$ mm, $L_g = 100$ mm, $th = 0.5$ mm, $tv = 1.2$ mm, $g = 0.5$ mm, $s = 4$ mm, and $t = 4$ mm. This antenna is best suited for GPS 1.5 GHz and 2.4 GHz WLAN applications. While Figure 3(b) depicts the dimensions of the top plane and the slot's edge.

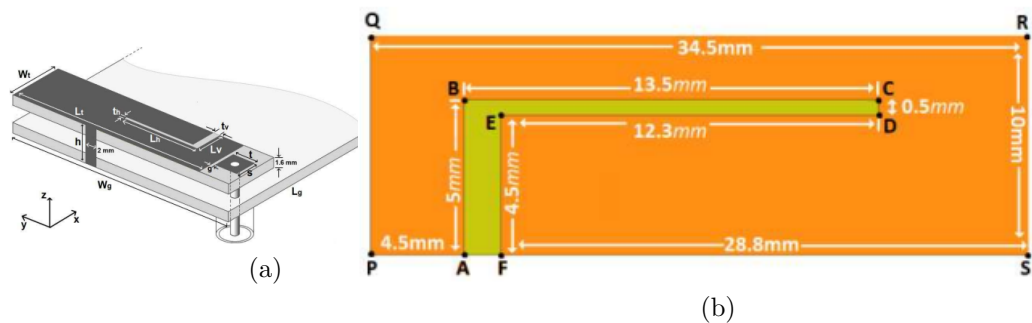


Figure 3: (a) Geometry of the proposed PIFA, (b) Dimension of top plane.

3 Results and Discussion

After the previous discussion on antenna design, this section will discuss the results of antenna measurements and simulations.

3.1 Planar Inverted-L Antenna (PILA)

A compact Triple-band PILA antenna [6], is simulated using the HFSS simulator. The proposed antenna prototype was made to verify the simulation results. S_{11} was measured using the 9916A Agilent Network Analyzer. The simulation results and measurements show that parameter S_{11} is $S_{11} \leq -10$ dB and the gain variation in each operating band is less than 1 dB. Radiation patterns were measured in the E plane (X-Z plane) and H plane (Y-Z plane) at 2.3 GHz, 5.4 GHz, and 8.3 GHz and show that they are nearly omnidirectional in the H plane and figure eight in the E plane at 2.3 GHz. The radiation pattern becomes directive at 5.4 GHz because the parasitic element acts as a guide at 5.4 GHz. Simulation and optimization of a compact four-band cactus-shaped antenna [7], were carried out using the commercial software ANSYS HFSS. The measured and simulated reflection coefficient S_{11} produces $S_{11} \leq -10$ dB. In addition, the impedance bandwidth of 10 dB for the four bands is 150 MHz (2.10 GHz–2.25 GHz), 400 MHz (3.25 GHz–3.65 GHz), 1022 MHz (4.42 GHz–5.44 GHz), and 1400 MHz (5.60 GHz–7.00 GHz), respectively. The radiation pattern and peak gain of the antenna, including the radiation characteristics, were measured in the anechoic chamber and the measurements were compared to a standard horn antenna. The normalized radiation patterns of the E-plane and H-plane at 2.15 GHz, 3.5 GHz, 4.8 GHz, and 5.8 GHz show that the cross-polarization in the E-plane is very good omnidirectional form. While in the H-plane the omnidirectional shape can also be well seen. Furthermore, the beam efficiency of the four frequency points of the antenna is very high, and a small side lobe appears only at the top. Such properties are preferred for cellular and WLAN communications. The peak gain over the 2 GHz–7 GHz frequency range is nearly 5 dB in the 5.60 GHz–7.00 GHz range.

Another PILA antenna [8], showing the reflection coefficient (S_{11}) measured on an Agilent N5234A PNAL network analyzer for simulation validation (S_{11}) on a CST MWS in an open environment is $S_{11} \leq -10$ dB which resonates at a frequency of 2.55/3.42/5.5 GHz with appropriate impedance bandwidths (IBWs) of 180 MHz (2.47–2.65 GHz)/360 MHz (3.27–3.63 GHz)/630 MHz (5.20–5.83 GHz) and FBW of 7.03/10.43/11.4%, respectively. Gain variations measured in the first band 1.76–2.38 dBi, the second band 1.78–2.35 dBi, and the

third band 1.69-2.39 dBi were found with gain variations less than ± 0.35 dBi, while the simulation gains of 2.0-2.72, 1.96-2.58, and 1.94-2.62 dBi were achieved in the 2.6 GHz, 3.5 GHz, and 5.5 GHz operating bands with each gain variation less than of ± 0.4 dBi. Comparison of normalized measurements together with simulated far-field patterns in the yz-plane ($= 90^\circ$) and xz-plane ($= 0^\circ$) at fr1 = 2.55, fr2 = 3.42, and fr3 = 5.5 GHz which produces an almost dipole-like co-polarization pattern at $= 90^\circ$ and an omnidirectional co-polarization pattern at $= 0^\circ$ in the yz-and xz-planes, respectively. The cross-polarization pattern (X-pol) is slightly weaker as compared to the co-polarization pattern in the yz-and xz-planes and at frequencies fr1, fr2, and fr3, the co-pol and X-pol differences in the boresight direction are 16 dB in the yz plane, 12 dB in the xz plane, and 9 dB in the xz plane.

A compact ultra-wideband (UWB) antenna [9] has good impedance matching over the entire frequency range of 2.7-12.55 GHz. The impedance bandwidth is over 129% (2.7-12.55 GHz) for $-S_{11} < 10$ dB. Numerical parametric analysis via Ansoft HFSS was carried out to understand the effect of the physical dimensions of the antenna on the impedance bandwidth and to validate the numerical results obtained by Ansoft HFSS, the antenna was constructed and tested in an anechoic microwave chamber. At various frequencies, the antenna co- and cross-pole far-field radiation patterns were measured (H(x-z)-and E(y-z)-plane patterns at only 3, 7, and 12 GHz compared). The antennas provide nearly omnidirectional and bidirectional patterns in the H-and E-planes, respectively. In addition, the maximum measured antenna gain is 4.5 dBi, which occurs at 11 GHz, and the desired radiation efficiency is greater than 81% in the 3–12 GHz frequency range.

Table 3: Comparison Of The Results Of All Proposed Antennas

No	Ref	Reflection Coefficient	Gain	IBW	FBW	Radiation Efficiency
1	[6]	< -10 dB	< 1 dB			
PILA	[7]	< -10 dB	Nearly 5dB max	150 MHz (2,10 GHz–2,25 GHz)		
			@5.60–7.00 GHz	400 MHz (3,25 GHz–3,65 GHz)		
				1022 MHz (4,42 GHz–5,44 GHz)		
				1400 MHz (5,60 GHz–7,00 GHz)		
3	[8]	< -10 dB	$< 0,35$ dBi(measured) $< 0,4$ dBi(simulated)	180 MHz (2,47–2,65 GHz) 360 MHz (3,27–3,63 GHz) 630 MHz (5,20–5,83 GHz)	7.03/ 10.43/ 11.4%	
4	[9]	< -10 dB	4,5 dBi max @11GHz	129%		81% @3-12GHz
PIFA	[10]	< -10 dB	1,07 dBi @ 2.45GHz	4,7% @2,45 GHz		92% @ 2.45GHz
			3,36 dBi @5.5Ghz	9% @5,5 GHz		88% @5.5Ghz
6	[11]	< -10 dB	2,24 dBi @1,5 GHz 7 dBi @2,4 GHz	30MHz @1.5GHz 76MHz @2.4GHz		82% @ 1,5 GHz 95.8% @2,4 GHz

3.2 Planar Inverted-F Antenna (PIFA)

A dual-band PIFA [10] shows the measured and validated reflection coefficient on HFSS is $S_{11} < -10$ dB with a relative impedance bandwidth of 10 dB as measured by the reflection coefficient is 4.7% at 2.45 GHz (2.5 GHz to 2.62 GHz), and 9% at 5.5 GHz (5.28 GHz to 5.78 GHz). In addition, the calculated radiation efficiency is 92% and 88% at 2.45 GHz and 5.5 GHz, respectively, with calculated peak, and realized gains of 1.07 dBi and 3.36 dBi, respectively. Another PIFA antenna [11] was performed using the PNAE6362B network analyzer. The antenna far-field measurements were carried out in the anechoic chamber. The simulated and measured reflection coefficient curve of the proposed PIFA is $S_{11} < -10$ dB. The resonant frequency of 1.5 GHz has a bandwidth of 30 MHz and 2.4 GHz has a bandwidth of 76 MHz. The two-dimensional radiation pattern of the PIFA antenna in three principal planes for the two resonant frequencies of 1.5 GHz and 2.4 GHz offers an almost omnidirectional radiation pattern in both resonances. It is known that for lower resonances, cross-pole currents accumulate at the upper and lower edges of the ground plane. This is why the author got low cross-pole isolation for the first resonance at 1.5 GHz. In addition, the antenna offers a peak gain of 2.24 dBi in the 1.5 GHz operating band and 7 dBi in the 2.4 GHz operating band. The average radiation efficiency (simulation) is 82% in the 1.5 GHz operating band and 95.8% in the 2.4 GHz operating band.

4 Conclusion

The results of a review of the planar inverted antenna types conducted by many researchers found that the antenna designed by Juan Zhang et al. is the best solution that can be applied in mobile communication

systems. The antenna is designed to have a compact antenna dimension ($21 \times 29 \times 1.6$ mm³) and has four frequency bands, whereas other studies only have two or three bands, and some are operated on the UWB frequency band, where, as we know, the weakness of the UWB frequency is the short communication distance. According to the obtained frequency band, an antenna can be applied to (N1/N78/N79) 5G and 5.8 GHz WLAN. In addition, the antenna has a high gain of almost 5 dB in the 5.60–7.00 GHz frequency range. Furthermore, Juan Zhang et al. also claim that the antenna has a beam efficiency of four very high-frequency antenna points and a small side lobe that appears only at the top, which appears at the highest frequency point. Such properties are preferred for mobile communications. This is in accordance with the requirements of mobile communication technology, which wants to have a high-speed communication system (video streaming and downloading), then the antenna design must have high gain and efficiency, as well as an antenna designed for multiband, compact size, lightweight, and ease of manufacture. But unfortunately, the antenna cannot cover the entire frequency range that must exist in a mobile communication system.

References

- [1] A. S. Debele, "Review of Multiband Antenna for Mobile Communication," *J. Electr. Eng. Electron. Control Comput. Sci.*, vol. 7, no. 23, pp. 43–50, 2021.
- [2] Y. Nie and L. Song, "A compact triband fractal PIFA antenna for mobile handset applications," *Proc. 2013 6th Int. Congr. Image Signal Process, CISP 2013*, vol. 3, no. Cisp, pp. 1468–1472, 2013, doi: 10.1109/CISP.2013.6743906.
- [3] M. Li, S. W. Cheung, C. F. Zhou, Q. L. Li, and D. Wu, "A compact monopole antenna for smartphones," *2017 IEEE Antennas Propag. Soc. Int. Symp. Proc.*, vol. 2017-January, pp. 193–194, 2017, doi: 10.1109/APUS-NCURSINRSM.2017.8072139.
- [4] J. Xie, Y. Yu, and H. Zhang, "A compact multiband internal antenna for 4g mobile terminals on a support," *Proc. - 2014 6th Int. Conf. Comput. Intell. Commun. Networks, CICN 2014*, pp. 10–12, 2014, doi: 10.1109/CICN.2014.13.
- [5] F. Ahmed, M. H. M. Chowdhury, and N. Hasan, "A Compact Multiband Antenna for 4G/LTE and WLAN Mobile Phone Applications," *2016 3rd Int. Conf. Electr. Eng. Inf. Commun. Technol. iCEEICT 2016*, pp. 8–11, 2017, doi: 10.1109/CEEICT.2016.7873058.
- [6] A. Khade, M. Trimukhe, S. Jagtap, and R. K. Gupta, "A Circular Sector with an Inverted L Shaped Monopole Antenna for Tri-Band Applications," *Prog. Electromagn. Res. C*, vol. 118, no. January, pp. 177–186, 2022, doi: 10.2528/PIERC22010802.
- [7] J. Zhang, X. Liu, C. Wang, L. Gan, Y. Wang, and L. Sun, "Compact four-band cactus-shaped antenna for 5g and wlan applications," *Prog. Electromagn. Res. Lett*, vol. 98, no. May, pp. 155–163, 2021, doi: 10.2528/PIERL21052902.
- [8] A. Kumar, J. K. Deegwal, and M. M. Sharma, "Miniaturized multistubs loaded rectangular monopole antenna for multiband applications based on theory of characteristics modes," *Prog. Electromagn. Res. C*, vol. 92, no. February, pp. 177–189, 2019, doi: 10.2528/PIERC19022009.
- [9] A. Dastranj and F. Bahmanzadeh, "A compact UWB antenna design using rounded inverted L-shaped slots and beveled asymmetrical patch," *Prog. Electromagn. Res. C* vol. 80, no. January, pp. 131–140, 2018, doi: 10.2528/pierc17111702.
- [10] T. Hirano and J. Takada, "Dual-band printed inverted-F antenna with a nested structure," *Prog. Electromagn. Res. Lett.*, vol. 61, no. April, pp. 1–6, 2016, doi: 10.2528/PIERL16041202.
- [11] P. V. Vinesh et al., "A compact capacitive coupled dual-band planar inverted F antenna," *Prog. Electromagn. Res. C*, vol. 52, no. July, pp. 93–99, 2014, doi: 10.2528/PIERC14042501.
- [12] R. Varma and J. Ghosh, "Analysis and design of compact triple-band meandered PIFA for 2.4/5.2/5.8 GHz WLAN," *IET Microwaves, Antenna Propag.*, vol. 13, no. 4, pp. 505–509, 2019, doi: 10.1049/iet-map.2018.5646.
- [13] S. S. Alja'afreh, Y. Huang, and L. Xing, "A compact, wideband and low profile planar inverted-L antenna," *8th Eur. Conf. Antennas Propagation, EuCAP 2014.*, vol. no. EuCAP, pp. 3283–3286, 2014, doi: 10.1109/Eu-CAP.2014.6902529.
- [14] W. C. Chang and C. H. Ku, "The planar coupled-fed multiband antenna for mobile handset application," *Proc. - 2015 5th Int. Conf. Commun. Syst. Netw. Technol. CSNT 2015*, pp. 93–97, 2015, doi: 10.1109/CSNT.2015.209.
- [15] D. EL NABAOU et al., "Multiband Planar Inverted F Antenna (PIFA) for ISM, WLAN and WiMAX Applications," *Int. Conf. Comput. Wirel. Commun. Syst. 2019*, 2019, doi: 10.4108/eai.24-4-2019.2284080.